Studies of Linear C_nSe^- ($1 \leq n \leq 11$) Clusters Produced from Laser Ablation: Collision-Induced Dissociation and ab Initio Calculations

Hai-Yan Wang, Rong-Bin Huang, Hong Chen, Meng-Hai Lin, and Lan-Sun Zheng*

State Key Laboratory for Physical Chemistry of Solid Surface, Department of Chemistry, Xiamen University, Xiamen 361005, China

Received: November 28, 2000; In Final Form: February 20, 2001

Small carbon cluster anions doped with single selenium atom C_nSe^- ($n = 1$ to 11) were produced by laser ablating the mixture of selenium and carbon powders and were recorded by mass spectrometry. Distribution of the doped cluster ions was found to vary with the mixed ratios of the sample, but only the cluster with even number of carbon atoms could be produced in the experiment. Experiment of collision-induced dissociation (CID) verified molecular formulas of the selenium polycarbon clusters and found that they tend to lose a Se atom (for smaller size) or a CSe unit (for larger size). To examine the odd/even alternation effect and other structural features, the cluster ions were further investigated by ab initio calculations with ROHF and B3LYP methods using 6-31G* basis set. Based on the studies of other C_nX^- clusters and statistical distribution of the C_nSe^- clusters, geometry of the clusters was assumed to be linear chain with the selenium atom locating at its terminal and was fully optimized in the calculation. The calculated total energy, vertical electron detachment energy and fragmentation energy, bond length, and other structural parameters exhibit the alternation effect, showing that C_nSe^- clusters with even n are more stable than the odd clusters, in a good consistency with the mass spectrometric observation. The structural difference between opposite parties of C_nSe^- is found to reduce following the increasing number of carbon atoms. The theoretical investigation also shows that electron correlation has to be considered in the calculation and the result obtained by the density function method is sufficient to describe the structural features of C_nSe^- clusters. Besides, dissociation energies of six dissociation channels, losing C, C_2, C_3, CSe, C_2Se, or Se fragment, were calculated for C_nSe^- anions and the result also exhibits the parity effect and matches well with the CID experimental observation.

I. Introduction

Because of the discovery[1] and successful preparation[2] of C_{60}, carbon clusters, especially those with large sizes such as fullerenes, have been extensively studied both experimentally and theoretically in the past decade.[3−11] Meanwhile, the small carbon clusters have also attracted much attention in recent years.[12−17] Such an interest is partly due to the involvement of these species in the interstellar medium, which is in the quasi-collisionless conditions. Under these conditions, the small carbon clusters are formed by adding heteroatoms such as nitrogen, oxygen, sulfur, boron, or silicon,[18] which presents a variety of stability to the carbon chain. The carbon cluster anions containing a heteratom, C_nX^- (X = H, B, F, Si, Cl, Ti, V, Cr, Fe, Ni, W, Zr, Cs, Rb, Al, N, P, As, Bi, S, et al.) were produced by laser ablating the proper samples.[19] Their abundance exhibits odd/even alternation, which varied with the number of clustering carbon atoms and the nature of the heteroatom.[19] It has been found in the observed time-of-fight (TOF) mass spectra that the signal intensities of some C_nX^- clusters, e.g., X = H, B, S, F, Al, with even n are stronger than those with odd n.[20]

Geometry of the small size carbon clusters, including those containing a heteratom, is generally believed to be linear.[9] Although Zhan et al. reported that some C_nX^- anions, such as, C_nB^-,[21] C_nP^-[10], and C_nN^-,[22] of larger n calculated with higher levels are slightly bent in their ground state, most of the structural features calculated in the bent geometry do not exhibit significant difference with those computed with linear structure. However, computations made at much higher levels of theory (CCSD(T)) have revealed that C_nP^- ($n = 2-7$) clusters are linear.[23] Pascoli and Lavendy[24] also found that C_nN^- ($n = 2-7$) clusters are linear in their ground state. From these calculation results, it seems that the carbon clusters doped with single heteroatom are linear or nearly linear in their ground state.

The polycarbon sulfides C_nS and their protonated forms have recently been investigated both experimentally and theoretically.[25,26] Sulfur polycarbon hydride ions were generated by laser ablating the mixture of sulfur and carbon powder.[27,28] An odd/even alternation in signal intensities was observed, and the cluster cations with even size and the anions with odd size were absent in the recorded mass spectra. The computation results agree very well with the mass spectrometric observations.[28] Recently, the special properties and structural flexibility of $C_2S_m^-$ have been demonstrated with experimental and theoretical methods.[29] Because of the special properties of oxygen and sulfur, it is difficult to generate the C_nO^- or C_nS^- clusters which tend to react further with hydrogen or others to form more stable ions.

Following the study on the carbon clusters doped with sulfide atom, we have generated selenium polycarbon ions by laser ablating the mixture of selenium and carbon powder at the first time. Compositions of the cluster anions are determined by collision-induced dissociation of mass-selected ions. Different than the C_nO^- or C_nS^- clusters, the C_nSe^- cluster anions created in the experiment are relatively stable and can be observed by

* Author to whom correspondence should be addressed: E-mail: lszheng@xmu.edu.cn.

10.1021/jp004313s CCC: $20.00
Published on Web 04/21/2001

the mass spectrometer. Thus, although a variety of C_nX^- clusters have been previously studied, the C_nSe^- cluster anions have their special scientific significance. Herein we report the mass spectrometry and ab initio calculations of the C_nSe^- anions. The experimental and theoretical results are compared and correlated, and special attention is focused on the odd/even alternation effect of the clusters.

II. Experimental Section

The experimental technique has been previously described in detail,[30] so only a brief description will be given here. The selenium polycarbon ions, generated by laser ablating the mixture of selenium and carbon powders, diffused into the first accelerated region with their initial kinetic energy and then were accelerated by a pulsed field with a potential of 950 V. After flying through a 2.5 m field-free drift tube, ions with different masses were separated. The ions with a specific mass were then selected by a pulsed field (the "mass gate") and were decelerated to 50−200 eV in kinetic energy. At the entry of the second acceleration region, the mass-selected ions collided with a crossed supersonic molecular beam. Both parent and daughter ions after the collisions were accelerated by the second pulsed field with a total potential of 4000 V and analyzed by the second TOF-MS with a 1.5 m field-free drift tube.

The second harmonic output of a Quant-Ray Nd:YAG laser, with wavelength of 532 nm and pulse width of 7 ns, was used for creating the cluster ions. The power density irradiating on the sample surface was at the order of 10^8 W cm^{-2} after being gently focused by an 80 cm focal-length lens. The mass resolution of the first TOFMS exceeds 400 and about 100 for the second. During the experiment, the apparatus was running under a vacuum of 10^{-4} Pa. The back pressure of the colliding gas, highly purified nitrogen, was 2−4 atm. Pulse width of the molecular beam is less than 300 μs. To ensure that the nitrogen would not be involved in the reaction in the collision process, argon gas in high purity was also applied as the colliding gas in the dissociation experiment and the same colliding products were observed.

The sample, mixed carbon and selenium powders, which are of spectrometric purity, were pressed into the sample holder after being well mixed. It was found that the different mixed ratios affected the mass distribution of the product ions significantly.

III. Experimental Results

1. Mass Distribution. The selenium-doped carbon clusters anions were produced from laser ablation of mixed powder of selenium and carbon, but composition distribution of the clusters can be affected by the ratio between the two elements. The time-of-flight mass spectrum of Se_n^- and C_nSe^- (n = even) shown in Figure 1 was generated from a sample with a ratio of 20:1 (Se/C). Other mixing ratios have also been tried as the sample, but all of them unfavor the production of the doped clusters. No matter whichever ratio and other experimental condition have been tried, no C_nSe^- with odd n, the number of carbon atoms, could be produced in the laser ablation experiment.

The odd/even alternation effect of C_nSe^- ions suggests that the cluster ions with an even number of carbons are much more stable. The alternation effect has also been observed for the carbon chain doped with various heteroatoms.[9,10,14,20,31] For instance, a similar situation has been found for C_nB^-[31] and a completely opposite situation has already been observed for C_nN^-, in which only the ions with an odd number of carbons can be produced in the experiment.[14] The alternation effect

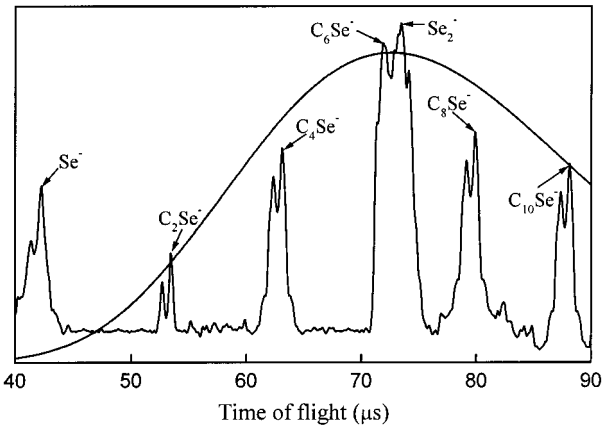

Figure 1. Mass spectrum of C_nSe^- generated from laser ablating a mixture of selenium and sulfur powders with the ratio of 20:1. The size distribution of clusters is fitted to a log-normal curve.

TABLE 1: Populations of the Fragment Ions from C_nSe^- with Even n (n = 2−10) Produced by Collision-Induced Dissociation[a]

parent anions	fragment ions and their relative abundance						
C_2Se^-	C_2^- (66)	C^- (34)					
C_4Se^-	C_4^- (46)	C_3^- (42)	C_2^- (12)				
C_6Se^-	C_2Se^- (3)	C_6^- (28)	C_5^- (45)	C_4^- (13)	C_3^- (11)		
C_8Se^-	C_4Se^- (4)	C_8^- (22)	C_7^- (42)	C_6^- (10)	C_5^- (8)	C_4^- (14)	
$C_{10}Se^-$	C_6Se^- (3)	C_{10}^- (20)	C_9^- (38)	C_8^- (12)	C_7^- (8)	C_6^- (15)	C_5^- (4)

[a] The relative abundance of each daughter ion is presented as a percentage of the depleted parent ions. Losing a selenium atom (for ions with smaller size) or a CSe unit (for larger size) is the main dissociation channel.

observed in mass spectrometry has been analyzed by the theoretical calculation, which is also applicable to the C_nSe^- system.

In addition, relative abundance of the C_nSe^- (n = even) anions can be well fitted by a log-normal distribution curve. According to the statistical distribution approach,[32] the distribution indicates that the C_nSe^- clusters have analogous structure, which is most probably the linear chain with the selenium atom locating at the end of the chain, like other doped carbon clusters.[9,10,14,31] In the mass spectrum, there is a doublet structure of the observed peak for each species, due to the two main isotopes of Se (^{78}Se, ^{80}Se). Also because of the mutual interference of the six isotopes of selenium element, peak width of each species is relatively wide.

2. Collision-Induced Dissociation (CID). CID not only determines composition of the clusters but also helps to characterize their structures. Results from the experiment of C_nSe^- (n = even) ions are shown in Table 1. In the table, the relative abundance of each daughter ion is presented as a percentage of the total ion yield. As shown in the table, dissociation patterns of the clusters are very similar and most of the dissociation reactions revealed in the CID experiment can be summarized as the following fragmentation channels:

$$C_nSe^- \rightarrow C_n^- + Se$$

$$C_nSe^- \rightarrow C_{n-1}^- + CSe$$

For the clusters of small size, losing a selenium atom is their

C 1.7976 Se
(-0.283) (-0.717)

C 1.2646 C 1.7703 Se
(-0.303) (-0.125) (-0.572)

C 1.3174 C 1.2488 C 1.7639 Se
(-0.230) (-0.157) (-0.036) (-0.578)

C 1.2585 C 1.3350 C 1.2288 C 1.7613 Se
(-0.256) (-0.261) (0.405) (-0.359) (-0.529)

C 1.2695 C 1.2880 C 1.3029 C 1.2370 C 1.7546 Se
(-0.175) (-0.579) (0.422) (0.293) (-0.441) (-0.519)

C 1.2464 C 1.3366 C 1.2273 C 1.3306C 1.2302 C 1.7450 Se
(-0.191) (-0.469) (0.019) (0.084) (0.535) (-0.573) (-0.405)

C 1.3067 C 1.2546 C 1.3213 C1.2271 C 1.3342 C 1.2226 C 1.7627 Se
(-0.051) (-0.757) (0.566) (-0.140) (-0.032) (0.548) (-0.594) (-0.540)

C 1.2393 C 1.3503 C 1.2154 C 1.3520 C 1.2102 C 1.3547 C 1.2139 C 1.7586 Se
(-0.196) (-0.455) (-0.213) (0.249) (0.022) (-0.361) (0.920) (-0.809) (-0.158)

C 1.2437 C 1.3379 C 1.2247 C 1.3307 C 1.2295 C 1.3144 C 1.2562 C 1.2724 C 1.7142 Se
(-0.150) (-0.474) (-0.110) (0.299) (-0.156) (-0.338) (0.498) (0.070) (-0.299) (-0.340)

C 1.2384 C 1.3520 C 1.2137 C 1.2557 C 1.2066 C 1.3631 C 1.2029 C 1.3647 C 1.2070 C 1.7702 Se
(-0.188) (-0.449) (-0.238) (0.452) (-0.283) (-0.243) (0.242) (-0.421) (1.067) (-0.865) (-0.073)

C 1.2408 C 1.3450 C 1.2178 C 1.3456 C 1.2132 C 1.3472 C 1.2159 C 1.3338 C 1.2382 C 1.2910 C 1.6998 Se
(-0.162) (-0.461) (-0.180) (0.484) (-0.269) (-0.176) (-0.040) (-0.371) (0.723) (-0.095) (-0.192) (-0.262)

Figure 2. The geometries of C_nSe^- clusters ($n = 1-11$) in their ground states optimized with the ROHF method. The basis set used is the 6-31G* described in the text. The values in parentheses are the net atomic charges from the Mulliken population analysis.

C 1.8086 Se
(-0.383) (-0.617)

C 1.2801 C 1.7837 Se
(-0.412) (-0.065) (-0.523)

C 1.3028 C 1.2930 C 1.7487 Se
(-0.463) (-0.071) (-0.073) (-0.535)

C 1.2765 C 1.3360 C 1.2523 C 1.7604 Se
(-0.476) (-0.242) (0.749) (-0.547) (-0.484)

C 1.2871 C 1.3081 C 1.2922 C 1.2717 C 1.7433 Se
(-0.409) (-0.6059) (0.661) (0.492) (-0.663) (-0.476)

C 1.2762 C 1.3290 C 1.2553 C 1.3226C 1.2534 C 1.7501 Se
(-0.386) (-0.645) (0.256) (0.555) (0.528) (-0.870) (-0.438)

C 1.2824 C 1.3135 C 1.2776 C1.2865 C 1.2981 C 1.2663 C 1.7388 Se
(-0.344) (-0.790) (0.240) (0.410) (0.460) (0.278) (-0.825) (-0.430)

C 1.2764 C 1.3255 C 1.2567 C 1.3176 C 1.2566 C 1.3181 C 1.2549 C 1.7437 Se
(-0.332) (-0.751) (-0.015) (0.502) (0.336) (0.151) (0.436) (-0.925) (-0.402)

C 1.2803 C 1.3153 C 1.2708 C 1.2943 C 1.2852 C 1.2787 C 1.3004 C 1.2642 C 1.7352 Se
(-0.309) (-0.828) (0.097) (0.350) (0.219) (0.164) (0.303) (0.264) (-0.867) (-0.396)

C 1.2769 C 1.3229 C 1.2573 C 1.3150 C 1.2577 C 1.3143 C 1.2576 C 1.3146 C 1.2563 C 1.7389 Se
(-0.305) (-0.786) (-0.061) (0.527) (0.052) (-0.055) (0.332) (0.087) (0.401) (-0.929) (-0.375)

C 1.2796 C 1.3156 C 1.2675 C 1.2982 C 1.2782 C 1.2864 C 1.2897 C 1.2746 C 1.3011 C 1.2635 C 1.7324 Se
(-0.290) (-0.832) (0.049) (0.403) (0.138) (-0.027) (0.095) (0.184) (0.260) (0.266) (-0.875) (-0.370)

Figure 3. The geometries of C_nSe^- clusters ($n = 1-11$) in their ground states optimized with the B3LYP method. The basis set used is the 6-31G* described in the text. The values in parentheses are the net atomic charges from the Mulliken population analysis.

main dissociation channel, but for larger clusters, ejecting a CSe unit becomes the predominant channel.

Under our experimental conditions, probability of multistep collision and fragmentation cannot be excluded. In fact, products from multistep fragmentation were also observed, especially for the parent anions with larger size. After losing the selenium atom, daughter ions subsequently lose C_3 units as other bare carbon cluster ions.[33]

IV. Computational Details

All calculations in this study were carried out by using the GAUSSIAN 94 set of programs.[34] We employ 6-31G* basis

TABLE 2: ROHF/6-31G* Energies (au), $\langle S^2 \rangle$, Dipole Moments μ (Debye), and Rotational Constants *Be* (GHz) of C_nSe^- ($n = 1-11$)

C_nSe^-	E_n	ΔE_n	$\langle S^2 \rangle$	μ	*Be*
1	−2435.3335		0.7500	2.4597	14.9896
2	−2473.2079	−37.8744	0.7500	4.6471	4.3516
3	−2511.0430	−37.8351	0.7500	5.0822	1.8842
4	−2548.9030	−37.8600	0.7500	6.3333	1.0084
5	−2586.7324	−37.8294	0.7500	6.7051	0.6101
6	−2624.5856	−37.8532	0.7500	10.5018	0.4005
7	−2662.4139	−37.8283	0.7500	14.2293	0.2772
8	−2700.2665	−37.8526	0.7500	19.3258	0.2011
9	−2738.0889	−37.8224	0.7500	16.1731	0.1527
10	−2775.9481	−37.8592	0.7500	25.6210	0.1166
11	−2813.7666	−37.8185	0.7500	23.2570	0.0932

TABLE 3: B3LYP/6-31G* Energies (au), $\langle S^2 \rangle$, Dipole Moments μ (Debye) and Rotational Constants *Be* (GHz) of C_nSe^- ($n = 1 \sim 11$)

C_nSe^-	E_n	ΔE_n	$\langle S^2 \rangle$	μ	Be
1	−2437.3741		0.7558	3.3017	14.8083
2	−2475.4928	−38.1187	0.7543	5.7115	4.2736
3	−2513.5764	−38.0835	0.7677	6.5449	1.8680
4	−2551.6798	−38.1034	0.7591	8.3977	0.9950
5	−2589.7612	−38.0814	0.7770	9.1113	0.6025
6	−2627.8555	−38.0943	0.7641	10.3261	0.3944
7	−2665.9357	−38.0802	0.7867	10.8704	0.2748
8	−2704.0257	−38.0900	0.7693	11.9412	0.1995
9	−2742.1054	−38.0797	0.7974	12.3854	0.1504
10	−2780.1930	−38.0876	0.7745	13.3682	0.1162
11	−2818.2724	−38.0794	0.8093	13.7401	0.0921

sets to perform calculations at the ROHF level, the restricted open-shelled Hartree−Fock theory, and at the B3LYP level, the density functional theory with the exchange functional of Becke[35] and correlation functional by Lee et al.[36] Geometries of the molecules are considered to be linear in this work, as verified by the fact that all the frequencies are real. In fact, we have tried to optimize the structure of C_8Se^- with no symmetrical restriction, but the optimized geometry is very close to being linear. The total energies and rotational constants were calculated along with bond lengths, vibrational frequencies, and relative intensities. The expected values of the spin angular momentum quantum number $\langle S^2 \rangle$ were also computed to check spin contamination.

V. Computation Results and Discussions

In the computation, bond lengths of the linear C_nSe^- ($n = 1-11$) clusters have been optimized by use of ROHF, and B3LYP methods with 6-31G* basis set. Subsequently, the corresponding harmonic vibrational frequencies are evaluated at the same level through the single point calculation. In this work, ground states of all C_nSe^- alternate between $^2\Sigma$ (even n) and $^4\Sigma$ (odd n) states.

Figure 2 presents the optimized bond lengths and the net charges obtained from the Mulliken population analysis at the ROHF/6-31G* level, while Figure 3 presents the data at the B3LYP/6-31G* level. Table 2 lists the calculated total energies E_n of optimized structures, ΔE_n (which is defined as the difference of E_n and E_{n-1}), $\langle S^2 \rangle$, dipole moments, and rotational constants of C_nSe^- ($n = 1-11$) in the ground electronic states studied in this work by employing ROHF/6-31G* theory, while Table 3 lists the data at the B3LYP/6-31G* level. The difference between the results calculated at the two levels can be perceived by comparing the corresponding data in the tables.

1. Structures. As shown in Figure 3, which displays the computational results at B3LYP/6-31G* level, the length of the C−Se bond of the anions reduces monotonically with the number of carbon atoms. Although the trend can be observed in the clusters with either even or odd carbons, the C−Se bond in the C_nSe^- with even n is longer than that with odd n. With an increase of the carbon chain, the difference tends to be smaller. In other words, the structural difference between the clusters with opposite parity of carbon number is a monotonic function of cluster size, reducing with increasing carbon atoms. Examining bond length on the carbon chain also reveals the structural difference of opposite parity. In the carbon chain with even size, the C−C bond length alternates between 1.25 Å and 1.32 Å, leaving a terminal C−C bond fixed at about 1.276 Å. High conjugativity of the even carbon chain exhibits its stable structure, while the odd carbon chain does not have the conjugative structure.

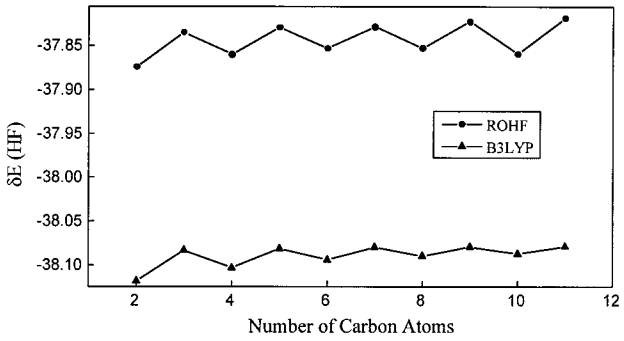

Figure 4. Calculated energy difference (in au) of linear C_nSe^- versus number of carbon atoms. The calculations were carried out at the ROHF/6-31G* and B3LYP/6-31G* levels.

The similar tendency can be found in the distribution of the negative charge density on the chain. The charge density on the selenium atom also reduces with increasing number of carbon atoms, while the charge density on the neighboring carbon atom increases correspondingly. Although the cluster anions with both even and odd number of carbon atoms exhibit similar tendency, the Se atom in odd cluster has higher charge density than that in even cluster, while the neighboring carbon in even cluster has relatively high charge density. Similarly, the difference reduces following increase of the cluster size.

It is noticeable that the structural features described above cannot be distinguished by the calculation at ROHF level, which result is displayed at Figure 2. In fact, the ab initio calculation at the level has been effectively applied to the carbon chain doped with nitrogen[14] or boron atoms.[31] The difference must be attributed to the greater number of electronic shells of the selenium atom compared with the nitrogen or boron atom, so that electronic interaction related to the selenium atom cannot be neglected. In the density functional theory, the exact exchange (HF) for a single determinant is replaced by a more general expression. The exchange-correlation functional includes terms accounting for both exchange energy and the electron correlation omitted in Hartree−Fock theory. Thus, with the most accurate hybrid density functional currently in use (B3LYP), DFT computations can lead to reliable geometries and harmonic frequencies at moderate costs.[37,38] So only the result calculated from the density functional theory could sufficiently describe the structural features of C_nSe^- clusters.

Although the total energy of each C_nSe^- cluster has been calculated at ROHF and B3LYP levels, it is impossible to evaluate the relative stability of the cluster with different size by simply comparing their total energies. For comparison, the energy difference ΔE_n, which can be readily obtained from the difference of the total energies between the adjacent clusters, is more effective. in Figure 4, the value of ΔE_n is displayed as

TABLE 4: Vibrational Frequencies (cm^{-1}) and Relative Intensities of Linear C_nSe^- ($n = 1-11$) Calculated by B3LYP/6-31G* [a]

C_nSe^-		
1	σ	785(18)
2	σ	641(3),2033(330)
	π	249(8),319(0)
3	σ	528(2),1400(26),1868(598)
	π	194(3),223(9),548(10),660(2)
4	σ	449(0),1100(27),1915(300),2156(38)
	π	151(9),155(6),416(12),430(6),844(0),874(0)
5	σ	405(3),955(84),1588(229),1930(1398),2017(12)
	π	104(5),106(7),292(7),297(10),547(1),613(0),1032(2), 1116(1)
6	σ	360(1),827(64),1322(29),1930(100),2116(944), 2162(219)
	π	79(5),80(4),226(10),230(8),440(2),446(0),728(1), 747(2),1338(0), 1360(0)
7	σ	333(3),747(115),1198(52),1682(1),1866(4465), 2013(7),2127(12)
	π	61(4),61(4),172(6),175(7),333(3),335(1),537(3),589(2), 834(0),894(0), 1584(1),1630(4)
8	σ	303(1),670(89),1071(17),1449(14),1933(741), 2074(29),2130(10), 2191(2194)
	π	48(4),49(3),139(6),140(5),267(3),267(4),445(4), 451(2),666(0),682(0), 999(0),1018(0),1845(0),1853(0)
9	σ	284(3),618(135),984(29),1344(54),1714(2070), 1812(5404),1984(35), 2119(794),2158(50)
	π	39(3),39(3),112(4),113(5),216(3),221(4)349(4),353(3), 517(0),563(0), 735(1),783(0),1100(0),1146(0)2029(0),2060(5)
10	σ	263(1),566(106),898(12),1226(40),1523(117),1934(245), 2040(83), 2062(2059),2185(181),2200(2864)
	π	33(3),33(3),93(4),94(4),183(3),183(2),286(4),292(5), 443(0),448(0), 614(1),628(1),844(0),861(0),1229(0),1238(0), 2192(0),2193(0)
11	σ	252(77),544(547),858(220),1163(1729),1428(8526), 1517(13066), 1818(2614),2184(2194),2225(7225),2370(2947), 2399(1046)
	π	26(5),27(5),78(3),78(3),154(2),155(3),247(3),249(3), 315(0),331(0), 510(0),575(0),689(2),718(1),917(2),954(8),1343(7), 1392(3),2378(0), 2417(44)

[a] The values in the parentheses are relative intensities.

a function of *n*, the number of carbon atoms. The characteristic odd/even alternation exhibits in the plot, evidencing the experimental observation very effectively.

Other structural parameters have also been calculated in the work. The inverse of the rotational constant is related to the bond lengths of a molecule and partially defines the box for the electrons. Interestingly, the Mulliken population analysis, shown in Figure 2 and Figure 3, can partly describe this trend. The rotational constants of C_nSe^- clusters are shown to decrease with the size of clusters, but the constant of each C_nSe^- cluster calculated at ROHF method is greater than that at B3LYP method. In contrast to the rotational constant, dipole moment of the linear molecule increases with length of the carbon chain as expected. Unlike the erratic data obtained at ROHF level, the dipole moment calculated at the B3LYP level is a monotonic function of carbon atoms, showing the characteristic odd/even alteration.

Spin contamination $\langle S^2 \rangle$ cannot be calculated by the ROHF method. The data obtained at B3LYP level shows that value of the parameter rises with increasing carbon atoms and the odd cluster has relatively high value. Contrary to the other structural parameters, the difference of the spin contamination between even and odd clusters increases with the cluster size.

To examine the true stability, the harmonic vibrational frequencies are calculated at the B3LYP/6-31G* level and are listed in Table 4. There is no imaginary frequency of all C_nSe^- ($n = 1-11$) ions, indicating that the linear geometries of C_nSe^- ions are indeed associated with the local minima on the potential energy surfaces.

2. Vertical Electron Detachment Energies. As is known, the ion signal intensity in a mass spectrum is related to the electron affinity or ionization energies of the molecule. The cluster ion with a larger ionization energy (or VDE) is generally more stable. Thus, vertical electron detachment energy (VDE), which is defined as the energy required to remove an electron from the anions without geometry change, is another criterion to evaluate the relative stability of the cluster anions with different sizes.

Table 5 lists VDE of C_nSe^- ($1 \le n \le 11$) anions calculated by using ROHF and B3LYP methods at 6-31G* level. The calculated data from both methods exhibit the dramatic odd/even alteration effect: The VDE of C_nSe^- with even *n* is larger than that of C_nSe^- with $n = n - 1$ or $n + 1$. The result implies that C_nSe^- anions with even *n* are more stable, in consistent with the experimental observation (Figure 1) that only C_nSe^- anions with even *n* were produced in laser plasma. Besides, the B3LYP data shows that the difference monotonically decreases with the number of carbon, but the trend cannot be distinguished in the ROHF data.

3. Fragmentation Energies. Relative stability of a series of clusters can be evaluated by the energy difference of the neighboring sizes of the cluster, which is, in chemistry, the reaction energy of

$$C_nSe^- \rightarrow C_{n-1}Se^- + C \quad (1)$$

Energy of the reaction is called the dissociation or fragmentation energy of C_nSe^-. Because of the existence of a selenium atom located at the end of the carbon chain, its possible dissociation channels are more complicated. Figure 5 and Figure 6 list the fragmentation energy calculated by ROHF and B3LYP methods for the six dissociation channels:

$$C_nSe^- \rightarrow C_{n-2}Se^- + C_2 \quad (2)$$

$$C_nSe^- \rightarrow C_{n-3}Se^- + C_3 \quad (3)$$

$$C_nSe^- \rightarrow C_{n-1}{}^- + CSe \quad (4)$$

$$C_nSe^- \rightarrow C_{n-2}{}^- + C_2Se \quad (5)$$

$$C_nSe^- \rightarrow C_n{}^- + Se \quad (6)$$

The six dissociation channels can be divided into two groups, losing small carbon particles C, C_2, or C_3, and losing CSe, C_2-Se, or Se fragment which consists of the heteroatom, Se. The dissociation energy of the latter is somewhat lower than that of the former, and losing CSe or Se fragment has the lowest energy, which matches very well with the result of CID experiment.

Fragmentation energy of ejecting carbon atom, the dissociation reaction 1, exhibits strong odd/even alternation with the

TABLE 5: Vertical Electron Detachment Energies (eV) of C_nSe^- ($n = 1-11$) Calculated by Employing the ROHF and B3LYP Methods at 6-31G* Level

method	CSe^-	C_2Se^-	C_3Se^-	C_4Se^-	C_5Se^-	C_6Se^-	C_7Se^-	C_8Se^-	C_9Se^-	$C_{10}S^-$	$C_{11}Se^-$
ROHF	0.140	2.715	1.246	3.112	1.959	3.425	2.831	4.178	2.957	4.825	3.572
B3LYP	0.204	3.130	1.371	3.437	2.130	3.659	2.608	3.820	2.949	3.914	3.196

cluster size, and the dissociation energy of C_nSe^- with even n is always larger than that of odd clusters. The result is consistent with the discovery that C_nSe^- with even n is relatively stable, because ejection of a single carbon atom will reverse the parity of the clusters and the more stable even cluster requires more energy to be fragmented to the less stable odd cluster.

On the other hand, losing a C_2 fragment will not change the parity of the parent cluster ions, so the alternation effect of the energy for reaction 2 should be less drastic than that of reaction 1 or 3. Since the even cluster is relatively stable, its dissociation will need slightly higher energy. It is just what is resulted from the calculation.

Dissociation energy of reaction 3 repeats the alternation tendency of the energy of reaction 1. However, the energy is found to be much less than that of reaction 1 or 2. The difference can be attributed to the special structural stability of C_3 fragment. In fact, ejection of C_3 has been found to be the major dissociation channel of small bare carbon cluster ions.[39] But in the experiments, the $C_{n-3}Se^-$ daughter ion was not observed, because the selenium atom is bound to the carbon chain much more loosely.

Dissociation energies of reaction 4, 5, and 6, which involve loss of selenium, exhibit the same alternation tendency, that is, the energy of C_nSe^- with even n is always larger than that of C_nSe^- with adjacent odd n. The C−Se bond of the doped carbon clusters is expected to be weaker than other C−C bonds, so the dissociation energy of reaction 6 is lower than those of other dissociation reactions. As the increase of the cluster size, the bonding interaction between carbon and selenium atoms gets stronger so as to weaken the adjacent C−C bond. Thus, for larger clusters, reaction 4 becomes the dominant dissociation pathway. The tendency is also shown in the calculated bond lengths of the clusters with an even number of carbons. As already shown in Figure 3, following the increase of the carbon chain, length of C−Se bond of the cluster gets shorter, while that of the C−C bond increases.

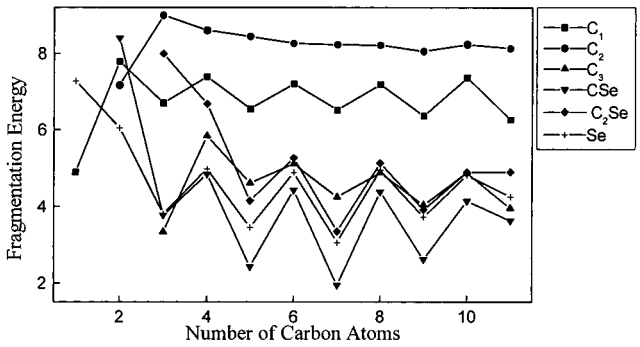

Figure 5. Fragmentation energies (eV) of C_nSe^- calculated by the ROHF/6-31G* method.

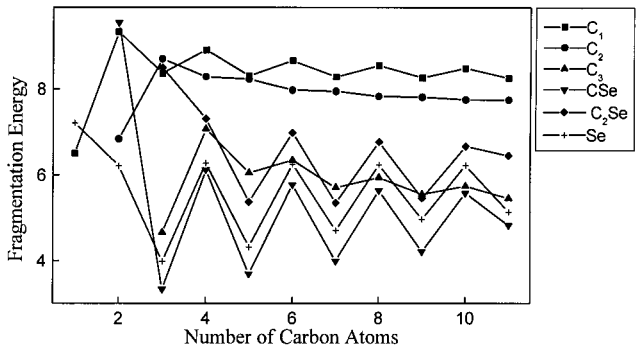

Figure 6. Fragmentation energies (eV) of C_nSe^- calculated by the B3LYP/6-31G* method.

Comparing the graphs in Figure 5 and Figure 6, it is easy to find that the dissociation energies computed at the different levels have no significant difference and exhibit a similar parity effect. However, the energy difference of the adjacent clusters illustrated in Figure 6 decreases monotonically with an increasing number of carbons, indicating that the distinctness of the clusters with different parities reduces following the growth of the carbon chain, while the tendency does not show in Figure 5. The comparison shows that B3LYP method is more sufficient to describe the structure of C_nSe^- clusters than ROHF method from another aspect.

The C_nSe^- ions were produced in the high temperature laser plasma. The species in the plasma have high internal energy and are expected to experience extensive dissociation reactions. Only the relatively stable species can survive from the reactions and finally be detected by the mass spectrometer. As a result, only the C_nSe^- clusters with even n, which have been shown to be more stable than the odd clusters, were finally recorded in the mass spectrum.

VI. Conclusion

C_nSe^- anions have been produced for the first time by laser ablation of mixed selenium/carbon powders with proper ratio. The following conclusions have been reached from experimental and theoretical studies of the clusters:

1. The C_nSe^- anions exhibit drastic odd/even alternation effect, which has also been observed in the other $C_nX^{\pm}$ ions, that is, the anions with an even number of carbon atoms are much more stable than those with an odd number. The effect was revealed from their special mass distribution, in which only the anions composed of an even number of carbon atoms have been recorded, and was verified by the various structural parameters, such as total energy, vertical electron detachment energy, fragmentation energy, and bond length, obtained from ab initio calculations. The calculation also found that the structural difference of the neighboring clusters monotonically decreases with the number of carbon.

2. The lowest-energy dissociation pathway of the small selenium polycarbon clusters is the ejection of the selenium atom and the C−C bond next to the selenium atom becomes the weakest bond as the length of the carbon chain increases. The discovery was reached by both CID experiment and ab initio calculation with excellent agreement.

3. From comparing the computational results obtained at different levels, it is found that ROHF/6-31G* level is not adequate for this C_nSe^- system, while the result calculated at B3LYP/6-31G* level can embody the structural features of the C_nSe^- clusters rather sufficiently.

Acknowledgment. This work was supported by the National Natural Science Foundation of China (Grant numbers 29890210, 29773040).

References and Notes

(1) Kroto, H. W.; Health, J. R.; O'Brien, S. C.; Curl, R. F.; Smalley, R. E. *Nature* **1985**, *318*, 162.

(2) Kratschmer, W.; Lamb, L. D.; Fostriropoulos, K.; Huffman, D. R. *Nature* **1990**, *347*, 354.

(3) Weltner, W., Jr.; Von Zee, R. J. *Chem. Rev.* **1989**, *89*, 1713.

(4) Zajfman, D.; Feldman, H.; Heber, O.; Kella, D.; Majer, D.; Vager, Z.; Naaman, R. *Science* **1992**, *258*, 1129.

(5) Watts, J. D.; Bartlett, R. J. *J. Chem. Phys.* **1992**, *97*, 3445.

(6) Hutter, J.; Luthi, H. P.; Diederich, F. *J. Am. Chem. Soc.* **1994**, *116*, 750.

(7) Forney, D.; Fulara, J.; Freivogel, P.; Jakobi, M.; Lessen, D.; Maier, J. P. *J. Chem. Phys.* **1995**, *103*, 48.

(8) Freivogel, P.; Fulara, J.; Jakobi, M.; Forney, D.; Maier, J. P. *J. Chem. Phys.* **1995**, *103*, 54.

(9) Moazzen-Ahmadi, N.; Zerbetto, F. *J. Chem. Phys.* **1995**, *103*, 6343.

(10) Sungyul Lee, *Chem. Phys. Lett.* **1997**, *268*, 69.

(11) Zhan, C. G.; Iwata, S. *J. Chem. Phys.* **1997**, *107*, 7323.

(12) Leleyter, M. *Z. Phys. D* **1991**, *20*, 81.

(13) Leleyter, M. *Z. Phys. D* **1991**, *20*, 85.

(14) Wang, C. R.; Huang, R. B.; Liu, Z. Y.; Zheng, L. S. *Chem. Phys. Lett.* **1995**, *237*, 463.

(15) Kishi, R.; Nakajima, A.; Iwata, S.; Kaya, K. *Proceedings for Yamada Conference* **1995**.

(16) Rodgers, M. T.; Armentrout, P. B. *J. Phys. Chem.* **1997**, *101*, 2614.

(17) Rodgers, M. T.; Armentrout, P. B. *J. Phys. Chem.* **1999**, *103*, 4955.

(18) Moazzen-Ahmadi, N.; Zerbetto, F. *J. Chem. Phys.* **1995**, *103*, 6343.

(19) Huang, R. B.; Wang, C. R.; Liu, Z. Y.; Qi, F.; Sheng, L. S.; Yu, S. Q.; Zheng, L. S. *Z. Phys. D* **1995**, *33*, 49.

(20) Vandenbosch, R.; Will, D. I. *J. Chem. Phys.* **1996**, *104*, 5600.

(21) Zhan, C. G.; Iwata, S. *J. Phys. Chem. A* **1997**, *101*, 591.

(22) Zhan, C. G.; Iwata, S. *J. Chem. Phys.* **1996**, *104*, 9058; **1996**, *105*, 6578.

(23) Pascoli, G.; Lavendy, H. *J. Phys. Chem. A* **1999**, *103*, 3518.

(24) Pascoli, G.; Lavendy, H. *Chem. Phys. Lett.* **1999**, *312*, 333.

(25) Ohshima, Y.; Endo,Y. *J. Mol. Spectrosc.* **1992**, *135*, 627.

(26) Hirahara, Y.; Ohshima, Y.; Endo,Y. *Astrophys. J.* **1993**, *L113*, 408.

(27) Liu, Z. Y.; Huang, R. B.; Zheng, L. S. *Int. J. Mass Spectrom. Ion Processes* **1996**, *155*, 79.

(28) Liu, Z. Y.; Tang, Z. C.; Huang, R. B.; Zheng, L. S. *J. Phys. Chem. A* **1997**, *101*, 4019.

(29) Chen, H.; Huang, R. B.; Lu, X.; et al. *J. Chem. Phys.* **2000**, *112*, 9606.

(30) Huang, R. B.; Liu, Z. Y.; Liu, H. F.; Chen, L. H.; Zhang, Q.; Wang, C. R.; Zheng, L. S.; Liu, F. Y.; Yu, S. Q.; Ma, X. X. *Int. J. Mass Spectrom. Ion Processes* **1995**, *151*, 55.

(31) Wang, C. R.; Huang, R. B.; Liu, Z. Y.; Zheng, L. S. *Chem. Phys. Lett.* **1995**, *242*, 355.

(32) Wang, C. R.; Huang, R. B.; Liu, Z. Y.; Zheng, L. S. *Chem. Phys. Lett.* **1994**, *227*, 103.

(33) Sowaresat, M. B.; Hintz, P. A.; Anderson, S. L. *J. Phys. Chem.* **1995**, *99*, 10736.

(34) Frisch, M. J.; Trucks, G. W.; Schlegel, H. B.; Gill, P. M. W.; Johnson, B. G.; Robb, M. A.; Cheeseman, J. R.; Keith, T. A.; Petersson, G. A.; Montgomery, J. A.; Raghavachari, K.; Allaham, M. A.; Zakrezewski, V. G.; Ortiz, J. V.; Foresman, J. B.; Cioslowski, J.; Stefanov, B.; Nanayakkara, B.; Challacombe, A. M.; Peng, C. Y.; Ayala, P. Y.; Chen, W.; Wong, M. W.; Andres, J. L.; Replogle, E. S.; Gomperts, R.; Martin, R. L.; Fox, D. J.; Binkley, J. S. GAUSSIAN 94; Gaussian, Inc.: Pittsburgh, PA, 1995.

(35) Becke, A. D. *Phys. Rev. A* **1988**, *38*, 3098.

(36) Lee, C.; Yang, W.; Parr, R. P. *Phys. Rev. B* **1988**, *37*, 785.

(37) Martin, M. L. J.; EI-Yazal, J.; Francois, J. P. *Phys. Lett.* **1995**, *242*, 570.

(38) Presilla-Marquez, J. D.; Tirrby, C. M. L.; Graham, W. R. M. *J. Chem. Phys.* **1997**, *106*, 8367.

(39) Raghavachari, K.; Birkley, J. S. *J. Chem. Phys.* **1987**, *87*, 2191.